A modular luminescence lifetime imaging system for mapping oxygen distribution in biological samples

Gerhard Holst [a,*], Oliver Kohls [a], Ingo Klimant [b], Bettina König [a], Michael Kühl [1,a], Thomas Richter [2,a]

[a] *Max-Planck-Institute for Marine Microbiology, Microsensor Research Group, Celsiusstr. 1, D-28359 Bremen, Germany*
[b] *Institute for Analytical Chemistry, Chemo- and Bio-Sensors, University of Regensburg, D-93040 Regensburg, Germany*

Abstract

We developed a new modular luminescence lifetime imaging system (MOLLI), that enables the imaging of luminescence lifetimes in the range of 1 µs to 1 s. The system can easily be adapted to different experimental applications. The central parts of the system are a recently released CCD-camera with a fast electronic shutter and gated LED (light emitting diode) or Xe excitation light sources. A personal computer controls the gating and image acquisition via a pulse delay generator. Here we present the new imaging system and give examples of its performance when used for measuring two-dimensional oxygen distributions with planar optodes. Furthermore, future applications of the system in biology are discussed. © 1998 Elsevier Science S.A. All rights reserved.

1. Introduction

Imaging of two-dimensional solute distributions with luminescent indicators has become an important tool in medicine, biology and physics. Most of the described image measuring systems and experimental setups were designed for specific applications like measurements of oxygen distribution in tissue [1–5], pH and Ca^{2+} distribution in cells [6,7], oxygen partial pressure on skin surfaces or oxygen flux into skin [8,9], oxygen distribution across the water-sediment interface [10] and in biofilms [11]. These setups were optimised for the corresponding experimental situation, but they lack versatility and many of them were e.g. confined to microscope setups [12–17]. Furthermore, imaging systems for time- and frequency-domain measurements often consist of complicated and rather bulky setups, using lasers as light sources, optical modulators, and sensitive slow scan CCD-cameras combined with fast gatable image intensifiers.

New bright semiconductor light sources, light emitting diodes (LED), that emit in the blue and blue-green part of the spectrum, offer a much cheaper and simpler alternative for a fast modulated or gated light source as compared to lasers. Furthermore, a recently developed sensitive and fast gateable CCD-camera simplifies lifetime imaging as it allows fast gating directly on the photosensitive chip. The image is digitised in the camera, and can be read out with the camera control board. An additional frame grabber is thus obsolete. We combined these new technologies with a trigger controller and a personal computer (PC) to develop a modular imaging system, which can easily be adapted to various applications. Here we describe the new imaging system and show its performance in applications where two-dimensional O_2 distributions are mapped via lifetime imaging of planar O_2 optodes.

---

* Corresponding author. Tel.: +49 421 2028834; fax: +49 421 2028690; e-mail: gholst@mpi-bremen.de
[1] Present address: Marine Biological Laboratory, University of Copenhagen, Strandpromenaden 5, DK-3000 Helsingør, Denmark.
[2] Present address: Institute for Biology II, Schänzlestr. 1, D-79104 Freiburg, Germany.

Table 1
Overview of different luminescence lifetime imaging methods

Lifetime detection	Procedure	+	−	Source
Frequency domain method	Sinusoidal modulation and phase angle shift	Better separation of different species with similar lifetimes	Complex setups (that need an image intensifier for sinusoidal modulation of gain), good optical filtering necessary	[26,25,28]
Ratioing method	Rectangular modulation and ratioing	Higher signal-to-noise ratio than time-domain and fast calculation	Background luminescence cannot be separated, good optical filtering necessary	[9]
Time-domain method	Pulse and gate	Simple separation of high background with short lifetimes, simple optical filtering	Species with similar lifetimes are difficult to separate, background with long lifetimes is difficult to separate	[15,3,5,27]

2. Theory

2.1. Oxygen sensing [2,6]

The dynamic quenching of luminescence by oxygen [1,7–10,3,4,18,5,19–24,11] is the basis for the measurement of oxygen distributions in various systems. The applied sensors have a planar structure with the luminescent indicator embedded in a polymer matrix that is spread on a transparent support foil. The sensor area is imaged through an optical emission filter in the case of intensity images or directly in the case of lifetime images by lenses or imaging fibres coupled to a photosensitive CCD-chip of the camera. Each pixel on the CCD now monitors the light intensity either as the absolute luminescence light emission, or, with proper timing, a part of the luminescence decay curve.

The oxygen optodes were calibrated with a two component model of the Stern–Volmer equation [22]:

$$\frac{\tau}{\tau_0} = \frac{I}{I_0} = \frac{\tan(\Phi)}{\tan(\Phi_0)} = \frac{\text{frac}}{(1 + K_{SV} \cdot [O_2])} + (1 - \text{frac}) \qquad (1)$$

τ, I, Φ = decay time, intensity or measured phase angle in presence of oxygen, τ_0, I_0, Φ_0 = decay time, intensity or measured phase angle in absence of oxygen, frac = fraction of quenchable luminophore, K_{SV} = bimolecular quenching coefficient, $[O_2]$, oxygen concentration.

2.2. Image detection

Luminescence lifetime imaging has two major advantages over intensity based imaging. It allows a good contrast enhancement and background suppression of unwanted luminescence contributions in the image. If this background luminescence has a different decay time than the luminophore of interest it is possible to separate the two signals by lifetime imaging. Further, lifetime imaging does not depend on intensity variations due to photobleaching (if it does not take place faster than the image acquisition) or variable indicator con-

centrations, and calibration free sensing applications [5] are possible. Table 1 gives an overview of the different possible methods for lifetime imaging, their inherent advantages and disadvantages.

The presented camera can not be modulated sinusoidally for frequency-domain evaluation, which has an advantage if images of different luminophores with similar lifetimes should be separated [25,13,14]. The phase delay ratioing method by Hartmann et al. [8,9] is possible with the new camera. However, it is not suitable for our applications because there can be an enormous background luminescence in the natural systems investigated with the new imaging system.

The new system, therefore, measures luminescence in the time-domain via a so called pulse-gate method [15,3–5]. Fig. 1 shows the detection principle applied for each pixel. For excitation the light source is
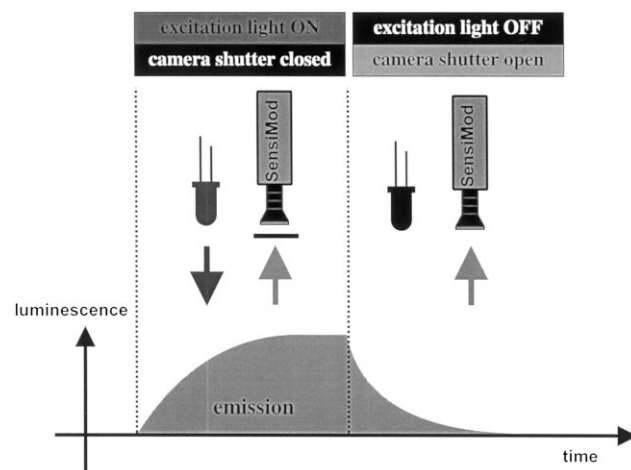

Fig. 1. Principle image acquisition timing scheme for luminescence lifetime imaging. The luminescence signal vs. time corresponds to the light signal that is detected by each pixel of the CCD-chip. The timing starts with excitation light 'on' and the camera shutter closed, the luminophore absorbs light and luminescence is emitted. Then the excitation light is switched 'off' and the camera shutter is opened with a possible delay.

luminescence
intensity

I_1

Δ

time

t_1
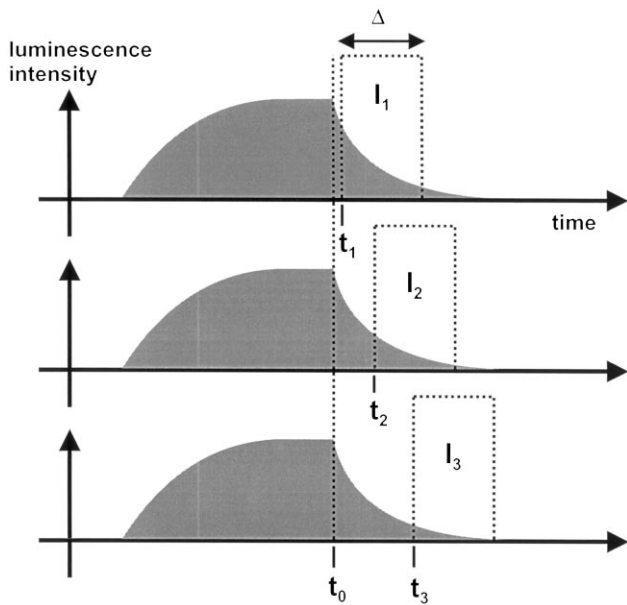
I_2

t_2

I_3

t_0 t_3

Fig. 2. Timing scheme for recording of images to evaluate the luminescence lifetime to generate lifetime images. All detected images have time windows of the same width Δ and integrate the intensity I_i of the decay curve. Each window has a different delay t_i compared to the switch 'off' time of the excitation light. To collect enough light, this window 'open' operation for a certain delay t_i is performed several hundred times and the light information is integrated on the CCD-chip.

switched 'on' and illuminates the planar optode, the arriving luminescence intensity increases until an equilibrium between absorbed and emitted energy of the dye molecules is reached. Then the light source is switched 'off' and the camera shutter is opened allowing luminescence and ambient light to reach the CCD-chip. This is repeated for a number of times, while incident light during the shutter open time is integrated on the CCD-chip before being passed to the PC. This procedure is repeated a couple of times to average the images and improve the signal-to-noise-ratio. To evaluate the corresponding lifetime of the light information detected by each pixel, three sets of images are collected, where each set is acquired with a different delay time t_i relative to the switch 'off' of the excitation light source.

The following image collection procedure is performed. Three sets of images ($i = 1, 2, 3$) are collected (see Fig. 2), while each image detection with a time interval Δ_i has a certain delay t_i compared to the excitation light 'off'. To receive enough light intensity, each image represents the integral over a number, n_i, of illumination events. The measured images S_i are stored.

The intensity of one image is given by:

$$I_i = \frac{S_i}{n_i}, \quad i = 1, 2, 3 \tag{2}$$

This intensity is, assuming a monoexponential decay curve with the apparent lifetime τ, described by the following equation:

$$I_i = I_0 \cdot \tau \cdot \exp\left(\frac{t_i}{\tau}\right) \cdot \left[1 - \exp\left(-\frac{\Delta_i}{\tau} \right) \right] \tag{3}$$

with the unknown intensity I_0 at time t_0 when the excitation light is switched 'off' (see Fig. 2). Instead of fitting the Values I_i to I_0 and τ we generate the new values:

$$W_1 = -\ln\left(\frac{I_1}{I_2}\right) \tag{4}$$

$$W_2 = -\ln\left(\frac{I_3}{I_2}\right) \tag{5}$$

If the image collection happens with the condition:

$$\Delta_1 = \Delta_2 = \Delta_3 = \Delta = \text{const.} \tag{6}$$

the new values give the following relations:

$$W_1 = \frac{t_1 - t_2}{\tau} \tag{7}$$

$$W_2 = \frac{t_3 - t_1}{\tau} \tag{8}$$

Therefore the lifetime per pixel can be directly calculated with the known delay times t_i:

$$\tau = \frac{(t_1 - t_2)^2 + (t_3 - t_2)^2}{W_1 \cdot (t_1 - t_2) + W_2 \cdot (t_3 - t_2)} \tag{9}$$

This method is not limited compared to a general fit to all values I_i. The generation of each value W_i (Eqs. (7) and (8)) with subsequent fit (Eq. (9)) do not yield to a principal deviation from a general fit as long as Eq. (6) is valid.

The calculation of the values (Eqs. (7) and (8)) has, by divison of the average values, the smallest error accumulation and is numerically stable. A variation of the timing window interval Δ, that is constant for all images, principally gives the opportunity to detect a non-limited number, n, of values to evaluate τ and, therefore, an error degression in the size of $1/\sqrt{n}$. This can be an advantage in the case of very noisy signals.

3. Experimental

3.1. Planar optode

The sensing layers for the comparison of luminescence intensity versus lifetime images were made of three different luminophores. The background or 'noise' layer was a commercial luminescent paint (Feuerrot, Conrad Electronics, Hirschau, Germany) with a luminescence decay time < 1 ns. This paint was spread on a microscope slide. The layers that should be

identified were made of two different oxygen indicators. One indicator was a Tris (4,7-diphenyl-1,10-phenantrolin)-ruthenium(II) perchlorate [8,9,22–24], dissolved in an organically modified sol-gel (ormosil) with dispersed titanium dioxide scattering particles. The other example was a platinum-octaethyl-porphyrine (Porphyrin Products, Utah, USA), dissolved in polystyrene that also can be used for oxygen determination. Both oxygen indicators were spread on microscope slides. For the oxygen measurement the ruthenium based sensor was knife-coated on a polyester foil that was cut to a size of 28×40 mm^2 to fit into the test setup.

3.2. Imaging system and application

The imaging system (Fig. 3) consists of an electrically cooled CCD-camera (SensiMod, PCO Computer Optics, Kehlheim, Germany) with a direct fast electronical shutter feature, due to a new and fast charge carrier transport from the light detection cell to the shift register, where the electrons can be accumulated until the picture frame is read out. Additionally, the camera has a special modulation input to control directly the fast shutter ($t_{on} = 500$ ns and $t_{off} = 500$ ns, maximum frequency = 1 MHz). The camera (dynamic range = 12 Bit, resolution = 640×480 pixel) is connected via a serial fibre-optical link to a camera control PCI-board in a Pentium based PC. The PC controls image acquisition, storage, display and the timing. For the precise timing of the excitation light source switching and image acquisition, the PC is connected via a GPIB interface to a delay pulse generator (DG535, SRS Stanford Research Systems, Sunnyvale, USA). Timing con-
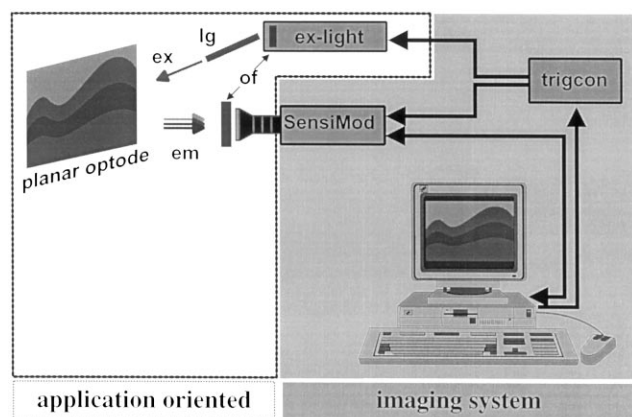

Fig. 3. Schematic overview of the modular luminescence lifetime imaging system. The imaging system consists of a fast gateable CCD-camera, SensiMod, a Pentium based PC, and a trigger control unit, trigcon. The application oriented part consists of the imaging object, planar optode, the excitation light source, ex-light, an optional light guide (lg) to transport the light to the imaging object, if necessary, optical filters (of). The emitted luminescence (em) reaches the camera via a lens.
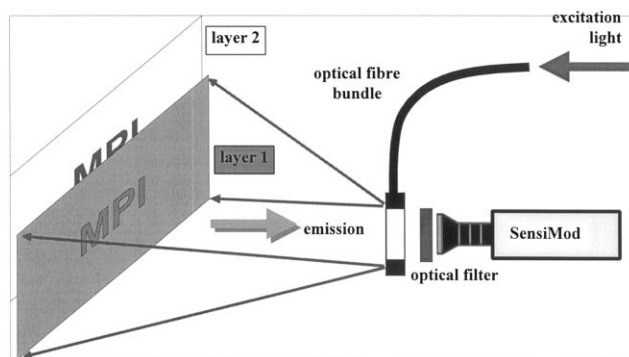

Fig. 4. Schematic drawing of the experimental setup for demonstrating the background suppression feature of luminescence lifetime imaging. The excitation light is coupled via fibre-optical ring light onto two different luminescent layers on microscope slides. The emission passes through the hole of the ring light, an emission filter (for the intensity images) and the lens to the CCD-camera.

trol und primary image aquisition was programmed in C (Watcom C/C + + 10 Compiler, Sybase, Emeryville, USA), while the image calculations and visualisation were programmed in a special software language made for the handling of large amounts of data (IDL 5.0, Research Systems, Boulder, USA).

For the experimental applications, the camera was equipped with a macro lens (Tevidon, F1.6/$f = 35$ mm, PCO) that imaged an area of 28×40 mm^2 onto the CCD-chip. This corresponds to a theoretical resolution of 50 μm pixel^{-1}. Two different light sources were applied for illumination, respectively excitation of the planar optodes. For lifetimes > 6 μs and luminophores with very low quantum efficiency, a Xenon flash lamp with adjustable output power and a maximum repetition rate of 30 Hz (A0021F, Oxygen Enterprises, Philadelphia, USA) was connected to a fibre-optical ring light, that was specially designed for the applications, i.e. a homogenous illumination of a circle of 50 mm diameter in a distance of 50 mm (Schölly Fiberoptic, Denzlingen, Germany). The second light source was developed for lifetime measurements from 100 ns upward and consists of up to 12 light emitting diodes ($\lambda_p = 470$ nm, BP280CWPB1K, DCL Components, Hungerford, UK), that are coupled into the same fibre-optical ring light. To enable fast switching of the LEDs, a special driving circuit with adjustable current was designed. The camera and the ring light were fixed in a special light tight housing, that can easily be applied to a vertically mounted sensing layer.

3.3. Experimental setups

For testing the luminescence background suppression, microscope slides were mounted in front of the camera setup (Fig. 4). The first strongly luminescent layer was the slide with the commercial paint, followed
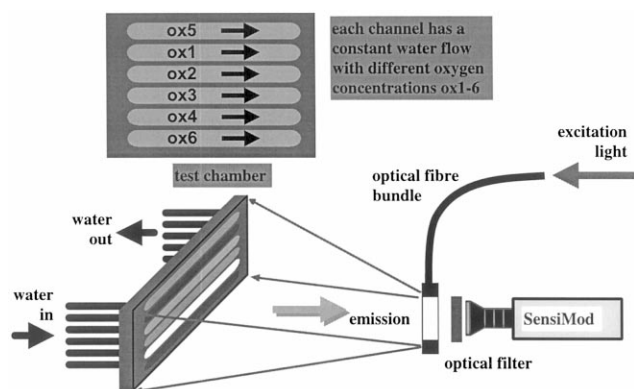
Fig. 5. Schematic drawing of the experimental setup for the oxygen mapping with planar optodes. A thermostated (not shown) test chamber with six perfusion channels was perfused separately by water with defined levels of dissolved oxygen (ox1–ox6). Towards the camera, the channel test chamber is closed with the planar optode pressed by a plastic window onto these channels. The chamber has a size of about 35×50 mm^2 to accept planar optodes of 28×40 mm^2. The excitation light again is coupled into a fibre-optical ring light as in Fig. 4.

by the slides with the two different oxygen indicators. To be able to compare the situations, the optical emission filter was kept at its position in front of the camera. The images were recorded with different timing between excitation light and camera.

For oxygen mapping, a special multichannel setup was designed with six different flow channels, that were connected to a peristaltic pump. Water with different oxygen concentrations can be guided through these channels, while the whole system is surrounded by a thermostating housing to keep the temperature constant. The planar optodes were pressed by a plastic window onto these channels and an outer o-ring (Fig. 5). Therefore, the system was closed towards the camera. Water was pumped from water bottles immersed in water with the same temperature as the test setup. The test water in the bottles was constantly flushed with nitrogen (Fig. 5, ox4), oxygen (Fig. 5, ox2) and room air (Fig. 5, ox1, ox3), and while channels 5 and 6 were filled with tap water and closed. In the results channel 5 (Fig. 5, ox5) cannot be seen because it was out of the camera field of view, which was adjusted for 50 μm pixel^{-1} resolution. Images were taken at 2 pixel vertical and horizontal binning, so the spatial image resolution was reduced to 100 μm pixel^{-1}.

4. Results and discussion

Fig. 6 shows the advantage of luminescence lifetime imaging in general. The pure intensity images (Fig. 6a, c) show a nearly constant grey distribution emphasising that the background luminescence is larger then the signal. Additionally, a lot of inhomogeneities can be
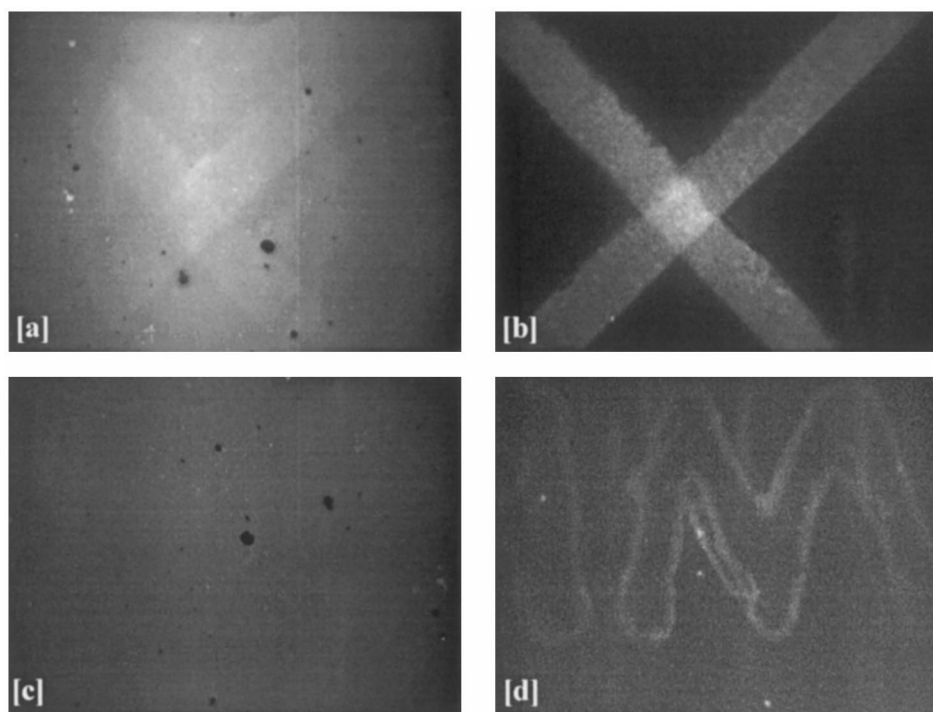

Fig. 6. Images of the background suppression tests, (a) and (c) are luminescence intensity images and (b) and (d) are delayed, decay curve proportional images. Layer 1 was for all cases a microscope slide with a fluorescent paint and layer 2 was in the upper case, a letter 'X' made of a ruthenium oxygen indicator (see text) with a decay time of 2.8 μs and in the lower case, a letter 'M' made of a porphyrine oxygen indicator with a decay time of ≈ 30 μs. The time delay of (b) was 1 μs and the delay of (d) was 4 μs.

seen (dark and white dots in Fig. 6a, c), that are due to the applied spreading procedure of the luminescence paint and some dirt on the microscope slide. When now the images are delayed by a certain time, t_d, the fluorescence of the paint is decayed while the two stripes forming a 'X' of the ruthenium indicator (Fig. 6b) as well as the drawn 'M' of the porphyrine compound (Fig. 6d) clearly can be detected.

The ruthenium based optode had a decay time at room air of about 2.8 µs, therefore, the delay of the image in Fig. 6b was $t_d = 1$ µs. The drawn 'M' with the porphyrine had a decay time of ≈ 30 µs, but the image taken with a delay time $t_d = 4$ µs (Fig. 6d) is not as high in contrast as the 'X'. This is due to the fact that the porphyrine has a lower quantum efficiency, a higher quenching coefficient compared to the ruthenium, and the sensing layer did not contain any additional scattering particles.

The results with the oxygen mapping setup clearly demonstrated that the test chamber needs further improvement (Fig. 7a to c). The images show no sharp channel structure. Obviously, oxygen diffused from the 100% channel (Fig. 5 ox2, the black one in Fig. 7a and b, the white one in Fig. 7c) into neighbouring channels (flow direction in Fig. 7 was from the left to the right), while the channel with zero oxygen (Fig. 5 ox4, the white one in Fig. 7a and b, the black one in Fig. 7c) received oxygen from the channels above and below (Fig. 5 ox3, ox6), respectively. Nevertheless, the lifetimes in the middle of the channels were in the same range as determined with single point measurements based on a phase modulation technique (i.e. $\tau_0 = 4.8 \pm 0.05$ µs, $\tau_{20} = 3.2 \pm 0.05$ µs, $\tau_{100} = 2.1 \pm 0.05$ µs for oxygen saturation of 0, 20, 100%, respectively).

Fig. 7 shows the luminescence intensity image with all associated imperfections, like texture within the sensing foil due to the knife coating process and the fast and difficult to control evaporation of the solvent of the ormosil. Additionally, some shadows can be seen, that are caused by water between the transparent window and the polyester support foil of the optode. Both phenomena are gone in the lifetime image (Fig. 7b), and the converted image of oxygen values (Fig. 7c), which represents an inversion of Fig. 7b because now the location of the most oxygen is white and the absence is black. The lifetime image was calculated both with a set of three delayed images and with four delayed images with a window at a width of $\Delta = 2$ µs and delay times of $t_1 = 500$ ns, $t_2 = 1$ µs, $t_3 = 2$ µs and $t_4 = 3$ µs, respectively. Additionally, a background blank image was subtracted with the same time window but with lights 'off', because the CCD-chip has a specific locally fixed noise distribution. Both fitting calculations resulted in the same lifetime distribution. This indicates the stability of the fitting procedure as well as the quality of the information gained within the
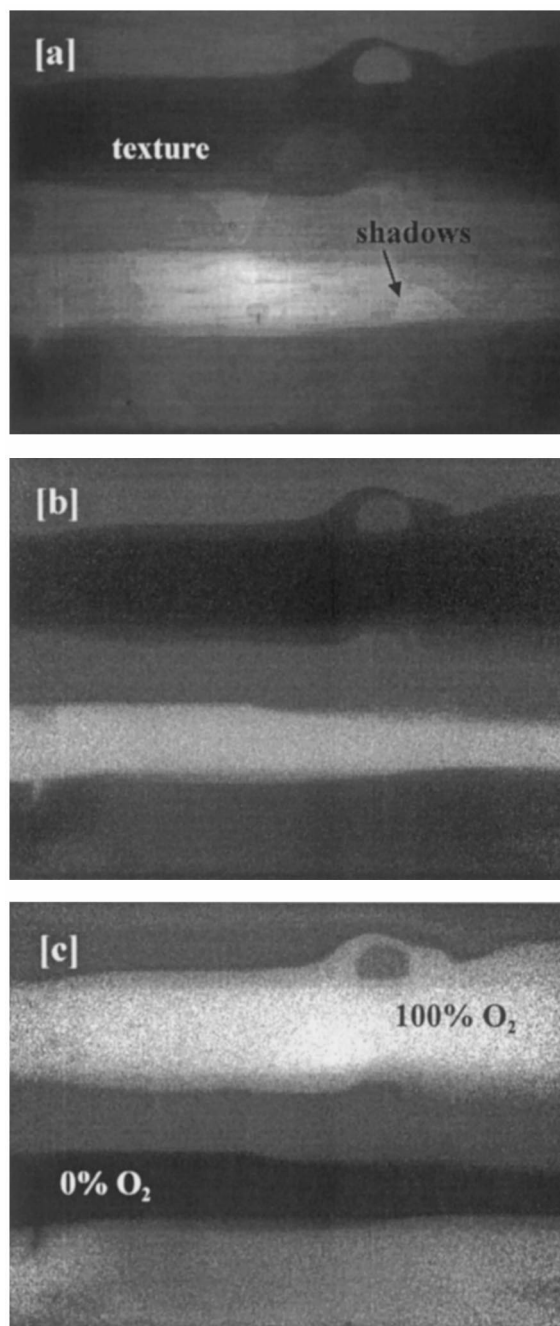

Fig. 7. Images with the oxygen mapping setup. Image (a) is an luminescence intensity image of the planar optode in the test setup with a certain texture of the sensing foil and some shadows due to an additional liquid layer in the setup between polyester support foil and terminating window. Image (b) is a luminescence lifetime picture evaluated by the described timing and calculation scheme, and image [c] is the corresponding oxygen image, that demonstrates the unwanted diffusion between each perfusion channel of the test chamber (see Fig. 5).

images. A 2 pixel vertical and horizontal binning was used for the oxygen mapping to increase the absolute signal range. We also took images without binning at full spatial resolution of 50 µm pixel^{-1}. Here the calculations gave the same lifetimes but resulted in

higher noise levels. The correspondence between the spatial image resolution per pixel, given by the camera chip and the lenses (either 50 or 100 μm pixel^{-1} in the demonstrated results), and the possible measuring resolution of the planar optodes has to be further investigated with specific test setups. This is necessary because of possible oxygen diffusion processes parallel to the optode surface, which could smear the spatial information.

5. Conclusion

A modular lifetime imaging system (MOLLI) based on a new, fast gateable CCD-camera was developed. This camera reduces the amount of equipment needed for lifetime imaging systems and allows for an easy adaption of the imaging system to different applications like optode based oxygen mapping in sediments and biofilms, around cells and aggregates.

Although the test setup for application of defined oxygen concentrations to the planar oxygen optodes was not optimum, the imaging system demonstrated the advantages of luminescence lifetime imaging in background signal suppression and less noise sensitive signal readout of planar optodes. This combined with the possibility of the measurement of two-dimensional distributions of solutes at high spatial resolutions instead of single profiles with microsensors the new system is a powerful tool for the investigation of natural biological systems.

Acknowledgements

References

[1] W.L. Rumsey, J.M. Vanderkooi, D.F. Wilson, Imaging of phosphorescence: a novel method for measuring oxygen distribution in perfused tissue, Science 241 (1988) 1649–1651.

[2] W.L. Rumsey, R. Iturriaga, D.F. Wilson, S. Lahiri, D. Spergel, Phosphorescence and Fluorescence Imaging: New Tools for the Study of Carotid Body Function, Chemoreceptors and Chemoreceptor Reflexes, Plenum Press, New York, 1990, pp. 73–79.

[3] R.D. Shonat, D.F. Wilson, C.E. Riva, M. Pawlowski, Oxygen distribution in the retinal and choroidal vessels in the cat as measured by a new phosphorescence imaging method, Appl. Opt. 31 (1992) 3711–3718.

[4] D.F. Wilson, S. Gomi, A. Pastuszko, J.H. Greenberg, Microvascular damage in the cortex of cat brain from middle cerebral artery occlusion and reperfusion, J. Appl. Physiol. 74 (1993) 580–589.

[5] S. Vinogradov, L.-W. Lo, W.T. Jenkins, S.M. Evans, C. Koch, D.F. Wilson, Noninvasive imaging of the distribution in oxygen in tissue in vivo using near-infrared phosphors, Biophys. J. 70 (1996) 1609–1617.

[6] J. Kavandi, J. Callis, M.P. Gouterman, et al., Luminescent barometry in wind tunnels, Rev. Sci. Instrum. 61 (1990) 3340–3347.

[7] M. Gouterman, Oyxgen quenching of luminescence of pressure sensitive paint for wind tunnel research, J. Chem. Educ. 74 (1997) 697–702.

[8] P. Hartmann, W. Ziegler, Lifetime imaging of luminescent oxygen sensors based on all-solid-state technology, Anal. Chem. 68 (1996) 4512–4514.

[9] P. Hartmann, W. Ziegler, G. Holst, D.W. Lübbers, Oxygen flux fluorescence lifetime imaging, Sensors and Actuators B 38–39 (1997) 110–115.

[10] R.N. Glud, N.B. Ramsing, J.K. Gundersen, I. Klimant, Planar optrodes: a new tool for fine scale measurements of two-dimensional O$_2$ distribution in benthic communities, Mar. Ecol. Prog. Ser. 140 (1996) 217–226.

[11] R.N. Glud, C.M. Santegoeds, D. DeBeer, O. Kohls, N.B. Ramsing, Oxygen dynamics at the base of a biofilm studied with planar optodes, Aquat. Microb. Ecol. 14 (1998) 223–233.

[12] J.R. Lakowicz, Fluorescence lifetime imaging sensing generates cellular images, Laser Focus World, 5 (1992).

[13] J.R. Lakowicz, H. Szmacinski, K. Nowaczyk, K.W. Berndt, M. Johnson, Fluorescence lifetime imaging, Anal. Biochem. 202 (1992) 316–330.

[14] H. Szmacinski, J.R. Lakowicz, M.L. Johnson, Fluorescence lifetime imaging microscopy: homodyne technique using high-speed gated image intensifier, Methods Enzymol. 240 (1994) 723–748.

[15] G. Marriott, R.M. Clegg, D.J. Arndt-Jovin, T.M. Jovin, Time resolved imaging microscopy, Biophys. J. 60 (1991) 1374–1387.

[16] R.M. Clegg, B. Feddersen, E. Gratton, T.M. Jovin, Time resolved imaging fluorescence microscopy, SPIE Conference on Time-Resolved Laser Spectroscopy in Biochemistry II (1990) 448–460.

[17] S. Nomura, M. Nakao, T. Nakanishi, S. Takamastu, K. Tomita, Real time imaging of microscopic pH distribution with a two-dimensional pH-imaging apparatus, Anal. Chem. 69 (1997) 977–981.

[18] R.L. Plant, D.H. Burns, Quantitative, depth-resolved imaging of oxygen concentration by phosphorescence lifetime measurement, Appl. Spec. 47 (1993) 1594–1599.

[19] H. Kautsky, Quenching of luminescence by oxygen, Trans. Faraday Soc. 35 (1939) 216–219.

[20] D.W. Lübbers, N. Opitz, The pCO$_2$/pO$_2$ optrode: a new probe for measuring pCO$_2$ and pO$_2$ of gases and liquids, Z. Naturforsch. 30C (1975) 532–533.

[21] I. Bergman, Rapid response atmospheric oxygen monitor based on fluorescence quenching, Nature 218 (1986) 396.

[22] J.R. Bacon, J.N. Demas, Determination of oxygen concentrations by luminescence quenching of a polymer immobilised transition-metal complex, Anal. Chem. 59 (1987) 2780–2785.

[23] I. Klimant, O.S. Wolfbeis, Oxygen sensitive luminescent materials based on silicone-soluble ruthenium dimiine complexes, Anal. Chem. 34 (1995) 3160–3166.

[24] I. Klimant, V. Meyer, M. Kühl, Fibre-optic oxygen microsensors, a new tool in aquatic biology, Limnol. Oceanogr. 40 (1995) 1159–1165.

[25] J.R. Lakowicz, K.W. Berndt, Lifetime-selective fluorescence imaging using a RF phase sensitive camera, Rev. Sci. Instrum. 62 (1991) 1727–1734.

[26] C.G. Morgan, A.C. Mitchell, J.G. Murray, Fluorescence decay time imaging using an imaging photon detector with a radiofrequency photon correlation system, SPIE Conference on Time-Resolved Laser Spectroscopy in Biochemistry II (1990) 798–807.

[27] X.F. Wang, T. Uchida, D.M. Coleman, S. Minami, A two-dimensional fluorescence lifetime imaging system using a gated image intensifier, Appl. Spec. 45 (1991) 360–366.

[28] R.M. Clegg, B. Feddersen, E. Gratton, T.M. Jovin, Time-resolved imaging fluorescence microscopy, SPIE Conference on Time-Resolved Laser Spectroscopy in Biochemistry III 1640 (1992) 448–460.

Biographies

Gerhard Holst, born 1962, studied electronical engineering at the RWTH University in Aachen, Germany, where he received the diploma in 1990, with a final work about reflectance pulse oximetry with electro-optical and hybrid fibre-optical sensors. From 1991 to 1994, he completed his Ph.D. in the group of Professor D.W. Lübbers at the Max-Planck-Institute (MPI) for Molecular Physiology, Dortmund, Germany, about a new optical chemical sensing principle, the oxygen flux optode and its phase modulation based measuring system. From 1994 he joined the microsensor research group of the MPI for Marine Microbiology, Bremen, Germany, as a post doc, where he is currently working on the development of new fibre-optic microsensors, microoptodes, their time resolved measuring schemes, and systems for laboratory and field applications.

Oliver Kohls, born 1965, graduated in technical chemistry at the University of Hannover, Germany, in 1992. In 1995 he received a Ph.D. at the University of Hannover. His work was about optical oxygen sensors, their measuring systems and their application in biotechnological process monitoring. Since 1995, he works in the MPI for Marine Microbiology in Bremen, Germany. His scientific interest is the development of optical microsensors and their application in the natural environment, especially marine systems.

Ingo Klimant, born 1964, graduated in analytical chemistry at the Bergakademie Freiberg, Germany in 1990. In 1993, he received a Ph.D. in chemistry from the Karl-Franzens University in Graz, Austria. His work involved the design of optical sensing schemes for oxygen and ammonia. From 1994 to 1996, he worked as a post doc at the MPI for Marine Microbiology in the microsensor research group and developed a variety of microoptodes for application in aquatic environment. Since 1996, he is at the Institute for Analytical Chemistry, Bio- and Chemical Sensors at the University of Regensburg, Germany. His scientific interest is the development of optical and optical chemical microsensors and their sensing schemes for application in biological systems.

Bettina König, born 1972, studied chemistry at the University in Regensburg, Germany, where she received the diploma in 1997 with a thesis about enzymatic determination of glucose by a combination of optode and microtiter plate techniques. From 1997 she joined the Microsensor Research Group of the MPI for Marine Microbiology, Bremen, Germany, as a Ph.D. student, where she is currently working on the development of new planar optodes and their application in biological environments.

Michael Kühl, born 1964, studied biology at the University of Aarhus, Denmark, where he received a M.Sc. degree in microbial ecology in 1988 with a thesis on the development of fibre-optic microprobes and a measuring system for microscale light measurements in sediments and biofilms. From 1988 to 1992, he completed his Ph.D. at the Department of Microbial Ecology, University of Aarhus, Denmark. His Ph.D. work involved the use of both optical and electrochemical microsensors to study the microenvironment in compact microbial communities. From 1992, he joined the MPI for Marine Microbiology, Bremen, Germany, as a post doc to build up microsensor research at the institute. From 1995 to 98 he was the head of the microsensor research group at the MPI in Bremen. Currently he holds a special research associate professorship at the Marine Biological Laboratory, University of Copenhagen, Denmark. His scientific interests are the development and use of fibre-optic and electrochemical microsensors in microbial ecology.

Thomas Richter, born 1962, graduated in mathematics (automorphic forms) and physics (negatively charged cluster ions) at the University of Freiburg, Germany, in 1987. In 1994 he received his Ph.D. at the University of Freiburg (Faculty of Biology). His work was about light propagation in higher plant leaves with a combined experimental and theoretical approach, including fibre-optic light measurements inside the leaf. He is working at the University in Freiburg on leaf photosynthesis and was a visiting scientist in microsensor research at the MPI from October 1997 to June 1998. His scientific interest concerns light driven processes in connection with ecological studies of photosynthetic performance in higher plants.